Inorganica Chimica Acta, 122 (1986) 37–44

Electrical Resistivities of Dibenzotetrathiafulvalene (DBTTF), Dibenzotetraselenafulvalene and Tetrathiatetracene Salts with Tin(IV) Hexachloride and Alkyltin(IV) (Alkyl = Me and Et) Chloride Anions, and X-ray Crystal Structure of $[DBTTF]_3[Sn_3Me_6Cl_8]\cdot PhCN$

RYUICHI SHIMIZU, GEN-ETSU MATSUBAYASHI and TOSHIO TANAKA*

Department of Applied Chemistry, Faculty of Engineering, Osaka University, Yamadaoka, Suita, Osaka 565, Japan

(Received June 5, 1986)

Abstract

Dibenzotetrathiafulvalene (DBTTF), dibenzotetraselenafulvalene, and tetrathiatetracene salts with tin(IV) hexachloride and alkyltin(IV) (alkyl = Me and Et) chloride anions were prepared by controlled current electrolyses of the donor molecules in solutions containing $[NBu^n_4]_2[SnCl_6]$ or SnR_2Cl_2 (R = Me or Et) and $[Ph_3PhCH_2P]Cl$. The obtained salts with $[SnCl_6]^{2-}$, $[SnMe_2Cl_3]^-$, $[SnEt_2Cl_3]^-$ and $[Sn_3Me_6Cl_8]^{2-}$ anions behave as typical semiconductors with electrical resistivities of $1\times(10^1-10^5)$ Ω cm at 25 °C as measured for compacted pellets. Electronic properties of the salts are discussed on the basis of infrared, electronic reflectance, and X-ray photoelectron spectra together with X-ray analysis. A single crystal X-ray structure analysis of $[DBTTF]_3[Sn_3Me_6Cl_8]\cdot PhCN$ showed that the salt contains a columnar structure consisting of a $DBTTF^{\ddagger}/DBBTF^{\ddagger}/DBTTF^0$ unit and a novel trimerized tin(IV) anion $[Sn_3Me_6Cl_8]^{2-}$. The crystals are triclinic, space group $P\bar{1}$, with cell dimensions $a = 12.931(2)$, $b = 20.992(4)$, $c = 12.485(1)$ Å, $\alpha = 90.07(1)$, $\beta = 99.18(1)$, $\gamma = 79.41(1)°$ and $Z = 2$. The least-squares refinement, based on 4183 independent reflections with $|F_o| > 3\sigma(F)$, converged at $R = 0.104$.

Introduction

In electrically conductive, organic sulfur- and selenium-donor salts, stackings of the donor radical cation (and molecules) may be influenced by geometries and formal charges of counter anions. Organometallic anions are of interest as the counter parts to prepare new organic radical cation salts because of their assuming some different geometries or formal charges. Recently, we reported the crystal structures and electrical properties of $[TTF]_3[SnR_2Cl_4]$ (TTF = tetrathiafulvalene; R = Cl [1], Me [2], and Et [3]), of which the salts with the dimethyl- and diethyltin(IV) tetrachloride anions involve a disorder with respect to the positions of the chlorine atom and the alkyl group and exhibit higher electrical conductivities than the $[SnCl_6]^{2-}$ analog without any disorders in the crystal structure [1].

Several years ago, $[DBTTF]_8[SnCl_6]_3$ (DBTTF = dibenzotetrathiafulvalene) was reported to exhibit a metallic conductivity [4]. Introduction of a disorder into the crystal structure of DBTTF salts by taking the $[SnR_2Cl_4]^{2-}$ (R = Me and Et) anion in place of $[SnCl_6]^{2-}$ is possible to afford new DBTTF packings. Thus, we have undertaken to prepare the salts of DBTTF and its selenium analog, DBTSF (dibenzotetraselenafulvalene), as well as TTT (tetrathiatetracene), with organotin(IV) chloride anions. This paper reports the preparations and electrical properties of DBTTF, DBTSF, and TTT salts with tin(IV) hexachloride and dialkyltin(IV) (alkyl = Me and Et) chloride anions as well as the packing modes of the donor moieties. A preliminary report of the X-ray structure of $[DBTTF]_3[Sn_3Me_6Cl_8]\cdot PhCN$ has appeared [5].

Experimental

Materials

Dibenzotetrathiafulvalene (DBTTF) [6], dibenzotetraselenafulvalene (DBTSF) [7], $[DBTTF]_5[BF_4]_4$ [8], tetrathiatetracene (TTT) [9], triphenylbenzylphosphonium chloride [3] and $[NBu^n_4]_2[SnCl_6]$ [10] were prepared according to the literature.

Preparation of DBTTF, DBTSF, and TTT salts

The electrolysis of an acetonitrile (10 cm^3) solution containing DBTTF (50 mg, 0.16 mmol), $SnMe_2Cl_2$ (990 mg, 4.5 mmol) and $[Ph_3PhCH_2P]Cl$ (580 mg, 1.5 mmol) under a constant current of *ca.* 5 μA for 10 d at room temperature afforded black plates of $[DBTTF]_{3.3}[Sn_3Me_6Cl_8]$ (1) (33 mg, 39% yield

*Author to whom correspondence should be addressed.

0020-1693/86/$3.50

TABLE I. Analyses and Melting Points of the DBTTF, DBTSF and TTT Salts

No.	Salt	Found (calc.) (%)			Melting point (decomp.) (°C)
		C	H	N	
1	$[DBTTF]_{3.3}[Sn_3Me_6Cl_8]$	36.55 (36.26)	2.71 (2.58)		>250
2	$[DBTTF]_3[Sn_3Me_6Cl_8]\cdot PhCN$	38.03 (37.83)	2.85 (2.71)	0.82 (0.80)	>238
3	$[DBTTF]_3[Sn_3Me_6Cl_8]\cdot PhNO_2$	37.69 (36.72)	2.75 (2.68)	0.61 (0.79)	>241
4	$[DBTTF]_{2.5}[SnEt_2Cl_3]\cdot 0.5MeCN$	45.16 (45.12)	2.82 (2.98)	0.58 (0.66)	>242
5	$[DBTSF]_{2.7}[SnCl_6]$	27.23 (27.28)	1.30 (1.31)		>273
6	$[DBTSF]_{2.5}[Sn_3Me_6Cl_8]$	25.03 (25.13)	2.31 (1.95)		>230
7	$[DBTSF]_4[Sn_3Me_6Cl_8]$	27.55 (27.60)	1.85 (1.87)		>285
8	$[DBTSF][SnEt_2Cl_3]$	27.58 (27.89)	2.18 (2.34)		>184
9	$[TTT]_{3.5}[SnCl_6]$	48.37 (48.35)	1.85 (1.80)		>328
10	$[TTT]_{1.3}[SnMe_2Cl_3]$	43.13 (43.07)	2.40 (2.32)		>250
11	$[TTT]_{1.5}[SnMe_2Cl_3]\cdot 0.75PhCN$	47.90 (47.77)	2.49 (2.55)	1.02 (1.22)	>239
12	$[TTT]_{1.5}[SnEt_2Cl_3]$	45.53 (45.86)	2.69 (2.73)		>222

based on DBTTF). Similarly, DBTTF was electrolyzed in benzonitrile and in nitrobenzene solutions containing excess amounts of $SnMe_2Cl_2$ and $[Ph_3PhCH_2P]Cl$ to give black columns of $[DBTTF]_3[Sn_3Me_6Cl_8]\cdot PhCN$ (**2**) (54% yield) and $[DBTTF]_3[Sn_3Me_6Cl_8]\cdot PhNO_2$ (**3**) (22% yield), respectively. Salt **2** was also obtained by the reaction of $[DBTTF]_5[BF_4]_4$ with excess amounts of $SnMe_2Cl_2$ in the presence of $[Ph_3PhCH_2P]Cl$ in benzonitrile [5].

DBTSF was electrolyzed in acetonitrile containing a large amount of $[NBu^n_4]_2[SnCl_6]$ as an electrolyte to give $[DBTSF]_{2.7}[SnCl_6]$ (**5**) (81% yield). The electrolysis of DBTSF in 1,1,2-trichloroethane and in acetonitrile by the similar method described for the DBTTF salts afforded $[DBTSF]_{2.5}[Sn_3Me_6Cl_8]$ (**6**) (45% yield) and $[DBTSF]_4[Sn_3Me_6Cl_8]$ (**7**) (49% yield), respectively.

$[DBTTF]_{2.5}[SnEt_2Cl_3]\cdot 0.5$ MeCN (**4**) and $[DBTSF][SnEt_2Cl_3]$ (**8**) were obtained by the electrocrystallization of DBTTF and DBTSF, respectively, in acetonitrile containing excess amounts of $SnEt_2Cl_2$ and $[Ph_3PhCH_2P]Cl$ (88 and 73% yields). Similar electrocrystallization of TTT in benzonitrile yielded $[TTT]_{3.5}[SnCl_6]$ (**9**), $[TTT]_{1.5}[SnMe_2Cl_3]\cdot 0.75PhCN$ (**11**), and $[TTT]_{1.5}[SnEt_2Cl_3]$ (**12**) (58, 82, and 83% yields, respectively). The use of acetonitrile as a solvent instead of benzonitrile afforded $[TTT]_{1.3}[SnMe_2Cl_3]$ (**10**) (71% yield).

The presence of the tin atom in those DBTTF, DBTSF, and TTT salts was confirmed by X-ray fluorescence analysis. The counter tin(IV) chloride anions of the salts were identified by far-infrared spectra. Elemental analyses and melting points (decomp.) of the salts are summarized in Table I.

Physical Measurements

Electrical resistivities were measured as compacted samples by the conventional two-probe method [11]. Powder electronic reflectance [12] and X-ray photoelectron spectra [13] were recorded as described elsewhere. Far–infrared (150–400 cm^{-1}) spectra were measured with an FIS-3 HITACHI far–infrared spectrophotometer. Cyclic voltammetric measurements of DBTTF and DBTSF were performed in a conventional cell consisting of a platinum working, a platinum counter, and a saturated calomel electrodes, using $[NBu^n_4]ClO_4$ as a supporting electrolyte in dichloromethane.

X-ray Data Collection

For a black plate of **2** prepared by electrocrystallization, accurate cell constants were determined by the least-squares treatment of the angular coordinates of independent 50 reflections with 2θ from 15 to 27°, measured on a Rigaku four-circle automated diffractometer with Mo Kα (λ = 0.71069 Å) radiation at Kwansei Gakuin University.

Crystal data

$C_{55}H_{47}Cl_8S_{12}Sn_3$, $M = 1746.1$, triclinic, space group $P\bar{1}$, $a = 12.931(2)$, $b = 20.992(4)$, $c = 12.485(1)$ Å, $\alpha = 90.07(1)$, $\beta = 99.18(1)$, $\gamma = 79.41(1)^\circ$, $U = 3287.4(9)$ Å^3, $Z = 2$, $D_c = 1.7460(5)$ g cm^{-3}, D_m (flotation) = 1.75 g cm^{-3}, $F(000) = 1724$, and μ(Mo Kα) = 12.2 cm^{-1}.

A specimen with dimensions 0.25 × 0.20 × 0.10 mm was used for the data collection. Intensity data were collected by the above-mentioned diffractometer using graphite-monochromatized Mo Kα radiation and a ω–2θ scan technique at a 2θ scan rate of 4° min^{-1}. The scan width in 2θ was $(1.0 + 0.34 \tan \theta)^\circ$. No significant intensity variation was observed throughout the data collection. The intensities were corrected for Lorentz and polarization effects. No correction was made for absorption. Of 6830 independent intensities measured in the range $2^\circ < 2\theta < 45^\circ$, 4183 reflections with $|F_o| > 3\sigma(F)$ were used for solving and refining the structure.

Solution and Refinement of the Structure

The positions of the tin atoms were indicated on a three-dimensional Patterson map. Subsequent cycles of Fourier syntheses and block-diagonal least-squares calculations gave a reasonable set of coordinates for the DBTTF molecules and the $[Sn_3Me_6Cl_8]^{2-}$ anion. However, the position of the solvent molecule, benzonitrile, included in the crystals, was disordered, the position of the terminal nitrogen atom being undetermined. The refinement was performed by assuming anisotropic thermal factors for the non-hydrogen atoms. No attempt was made to refine the hydrogen atoms. The residual indices in the final refinement was $R = \Sigma||F_o| - |F_c||/\Sigma|F_o| = 0.104$ and $R' = [\Sigma w(|F_o| - |F_c|)^2/\Sigma w|F_o|^2]^{1/2} = 0.141$, where the weighting scheme, $1/w = \sigma^2(F_o) + 0.001(F_o)^2$, was used. Atomic scattering factors used were taken from ref. 14. The final atomic coordinates with standard deviations are given in Table II. See also 'Supplementary Material'.

Crystallographic calculations were performed on an ACOS 900S computer at the Crystallographic Research Center, Institute for Protein Research, Osaka University. Figures 1 and 2 were drawn by the local version of the ORTEP-II program [15].

Results and Discussion

X-ray Crystal Structure of Salt 2

The crystal structure of salt **2** is shown in Fig. 1, which consists of the columnar array of the DBTTF‡ radical cations/DBTTF molecules and the $[Sn_3Me_6Cl_8]^{2-}$ anion. The disordered benzonitrile molecule is located between the DBTTF columns, though it is not illustrated in Fig. 1 for simplification. Figures 2 and 3 illustrate the overlapping modes of the

TABLE II. Atomic Coordinates (×10^4) for $[DBTTF]_3[Sn_3Me_6Cl_8]$PhCN (**2**) with Standard Deviations in Parentheses

Atom	*x*	*y*	*z*
Sn(1)	3248(2)	−1872(1)	1246(2)
Sn(2)	2243(2)	197(1)	895(2)
Sn(3)	1229(2)	2266(1)	546(2)
Cl(1)	3071(9)	−2771(6)	59(10)
Cl(2)	4252(9)	−2489(6)	2876(9)
Cl(3)	2113(8)	−835(5)	−350(8)
Cl(4)	3339(8)	−640(5)	2477(7)
Cl(5)	1200(8)	1018(5)	−671(8)
Cl(6)	2451(8)	1178(5)	2198(8)
Cl(7)	250(8)	2938(5)	−998(9)
Cl(8)	1500(9)	3134(6)	1819(9)
S(1)	1043(7)	711(5)	4219(7)
S(2)	576(7)	807(5)	6437(7)
S(3)	−1909(7)	1039(4)	5505(7)
S(4)	−1439(7)	928(5)	3293(7)
S(5)	218(8)	2419(5)	3900(7)
S(6)	−290(7)	2544(5)	6130(7)
S(7)	−2753(8)	2790(5)	5182(8)
S(8)	−2311(8)	2647(5)	2959(7)
S(9)	311(12)	4109(6)	3724(10)
S(10)	−1290(12)	4322(6)	5183(10)
S(11)	563(10)	4172(6)	7213(9)
S(12)	2166(10)	4009(6)	5779(10)
C(1)	1698(30)	−1774(22)	1717(29)
C(2)	4552(28)	−1652(18)	726(31)
C(3)	845(24)	104(19)	1394(31)
C(4)	3781(24)	277(21)	408(31)
C(5)	−120(28)	1980(22)	1132(24)
C(6)	2666(27)	2180(18)	35(27)
C(7)	2167(23)	637(16)	5188(24)
C(8)	3177(26)	498(21)	5040(32)
C(9)	4019(28)	433(18)	5955(33)
C(10)	3815(27)	528(17)	7000(30)
C(11)	2693(32)	625(20)	7178(25)
C(12)	1914(26)	692(18)	6320(24)
C(13)	113(22)	814(19)	5061(24)
C(14)	−968(28)	910(16)	4709(22)
C(15)	−2968(23)	1092(14)	4519(26)
C(16)	−3998(28)	1268(18)	4766(34)
C(17)	−4838(27)	1297(18)	3777(33)
C(18)	−4703(30)	1217(14)	2735(26)
C(19)	−3571(26)	1093(17)	2594(33)
C(20)	−2827(5)	1038(18)	3415(28)
C(21)	1263(27)	2376(16)	4954(27)
C(22)	2341(29)	2265(16)	4838(33)
C(23)	3124(32)	2222(21)	5685(32)
C(24)	2906(29)	2318(18)	6665(25)
C(25)	1885(32)	2411(15)	6930(26)
C(26)	1075(30)	2440(17)	6004(25)
C(27)	−691(28)	2522(24)	4741(30)
C(28)	−1806(30)	2632(18)	4386(24)
C(29)	−3889(32)	2896(19)	4143(28)
C(30)	−4955(31)	3067(20)	4361(35)
C(31)	−5742(32)	3121(19)	3402(33)
C(32)	−5531(31)	3005(23)	2384(35)
C(33)	−4474(32)	2944(19)	2182(32)
C(34)	−3643(29)	2835(18)	3121(29)

(continued)

TABLE II. *(continued)*

Atom	x	y	z
C(35)	−1076(32)	4167(19)	3029(32)
C(36)	−1796(34)	4289(20)	3756(32)
C(37)	−2879(39)	4399(21)	3516(50)
C(38)	−3251(45)	4393(25)	2352(50)
C(39)	−2481(39)	4252(26)	1641(40)
C(40)	−1376(39)	4149(19)	2031(30)
C(41)	12(31)	4188(19)	5031(29)
C(42)	838(36)	4142(18)	5874(35)
C(43)	2619(32)	3979(20)	7080(35)
C(44)	3690(53)	3839(24)	7431(45)
C(45)	4034(43)	3797(27)	8673(53)
C(46)	3358(59)	3997(40)	9277(48)
C(47)	2236(44)	4022(23)	9072(37)
C(48)	1965(37)	4057(19)	7883(36)
C(49)	1903(46)	5143(33)	1780(45)
C(50)	2566(39)	4760(21)	2457(39)
C(51)	3356(51)	5012(38)	3165(56)
C(52)	3768(50)	5497(25)	3261(52)
C(53)	3016(35)	5967(22)	2449(38)
C(54)	2238(43)	5921(25)	1652(45)
C(551)	1088(72)	5068(49)	950(60)
C(552)	1586(72)	5514(42)	1133(57)

C(49)–C(55): benzonitrile.

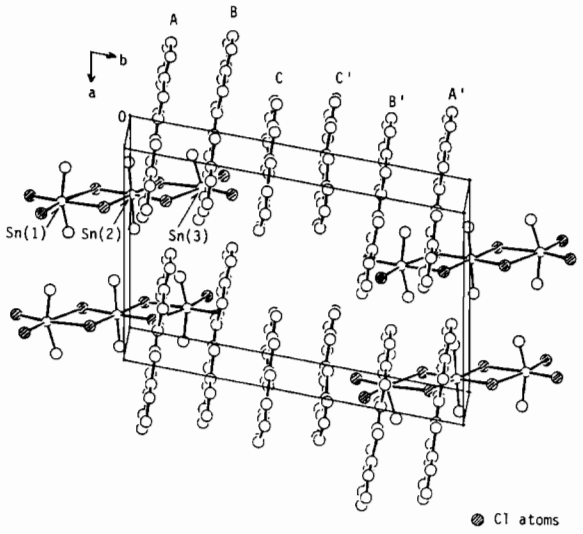

Fig. 1. Projection of the crystal structure of $[DBTTF]_3[Sn_3Me_6Cl_8]\cdot PhCN$ (2) along the c^* axis. The disordered benzonitrile molecules are not illustrated.

$DBTTF^{\ddagger}$ and/or $DBTTF^{0}$, and the $[Sn_3Me_6Cl_8]^{2-}$ anion, respectively, together with the atom-labelling scheme. The relevant bond lengths and angles are summarized in Table III.

DBTTF molecules are arranged as trimer units to form a column along the *b* axis. A trimer unit (A, B, and C) is located symmetrically to another

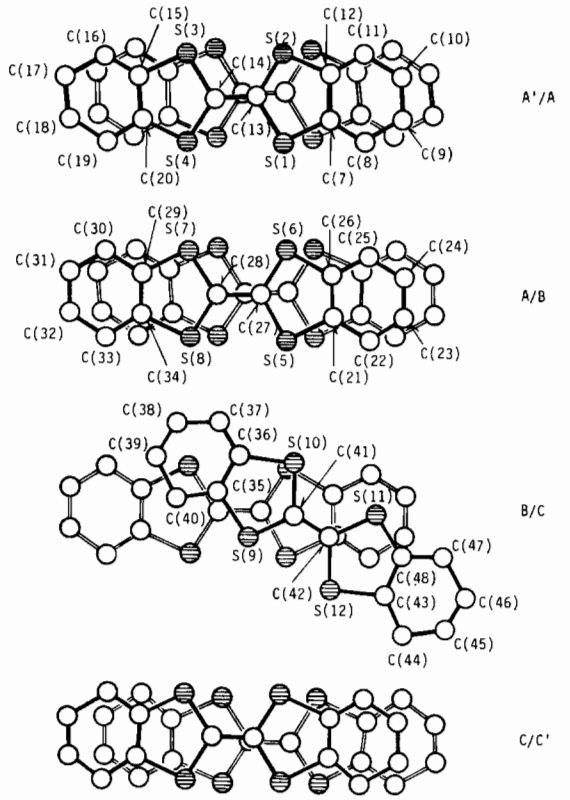

Fig. 2. Overlapping modes of the DBTTF molecules together with the atom-labelling scheme.

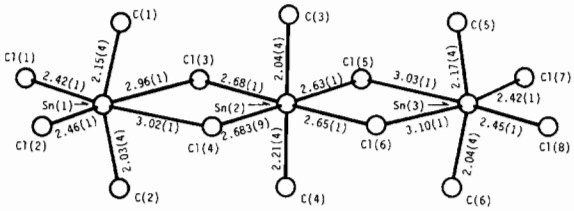

Fig. 3. The geometry of the $[Sn_3Me_6Cl_8]^{2-}$ anion together with the atom-labelling scheme and bond distances.

one (A′, B′, and C′). The spacings between the least-squares best planes within the column are 3.47 (A/A′); 3.51 (A/B), 3.52 (B/C), and 3.54 Å (C/C′), which are close to the molecular spacings of the metallic salt $[DBTTF]_8[SnCl_6]_3$ (3.44, 3.47, and 3.58 Å) [16] as a whole. Although the overlapping of (A/A′), (A/B), and (C/C′) is relatively sufficient, being similar to those of [DBTTF][TCNQ] [17] and $[DBTTF]_2[Cu_2Br_6]$ [18], the (B/C) overlap is insufficient. Probably for this reason, the salt exhibits a rather large electrical resistivity as described below. Of A, B, and C, the former two may be the $DBTTF^{\ddagger}$ radical cation and the latter neutral DBTTF, since the central C–C distance of molecule C (C(41)–C(42), 1.35(5) Å) is somewhat shorter than those of A (C(13)–C(14), 1.37(4) Å) and B (C(27)–C(28),

TABLE III. Selected Bond Distances (Å) and Angles (°) for $[DBTTF]_3[Sn_3Me_6Cl_8]\cdot PhCN$ (2) with Standard Deviations in Parentheses

S(1)–C(7)	1.72(3)	S(8)–C(28)	1.80(3)
S(1)–C(13)	1.71(3)	S(8)–C(34)	1.74(4)
S(2)–C(12)	1.73(4)	S(9)–C(35)	1.85(4)
S(2)–C(13)	1.73(3)	S(9)–C(41)	1.74(4)
S(3)–C(14)	1.67(4)	S(10)–C(36)	1.80(4)
S(3)–C(15)	1.68(3)	S(10)–C(41)	1.70(4)
S(4)–C(14)	1.78(3)	S(11)–C(42)	1.76(5)
S(4)–C(20)	1.80(4)	S(11)–C(48)	1.84(5)
S(5)–C(21)	1.72(3)	S(12)–C(42)	1.71(5)
S(5)–C(27)	1.68(4)	S(12)–C(43)	1.63(4)
S(6)–C(26)	1.77(4)	C(13)–C(14)	1.37(4)
S(6)–C(27)	1.73(4)	C(27)–C(28)	1.42(5)
S(7)–C(28)	1.68(4)	C(41)–C(42)	1.35(5)
S(7)–C(29)	1.17(4)		
S(2)--Cl(5)	3.49(2)		
Cl(1)–Sn(1)–Cl(2)	98.5(4)	S(3)–C(14)–S(4)	116(2)
C(1)–Sn(1)–C(2)	162(2)	S(3)–C(14)–C(13)	126(2)
Cl(3)–Sn(1)–Cl(4)	76.1(3)	S(4)–C(14)–C(13)	119(3)
Cl(3)–Sn(2)–Cl(4)	86.9(3)	S(3)–C(15)–C(20)	120(2)
C(3)–Sn(2)–C(4)	178(1)	S(4)–C(20)–C(15)	111(2)
Cl(5)–Sn(2)–Cl(6)	89.9(3)	S(5)–C(21)–C(26)	120(3)
Cl(5)–Sn(3)–Cl(6)	74.9(3)	S(6)–C(26)–C(21)	114(3)
C(5)–Sn(3)–C(6)	159(2)	S(5)–C(27)–S(6)	120(2)
Cl(7)–Sn(3)–Cl(8)	98.1(4)	S(5)–C(27)–C(28)	124(3)
C(7)–S(1)–C(13)	98(2)	S(6)–C(27)–C(28)	116(3)
C(12)–S(2)–C(13)	96(1)	S(7)–C(28)–S(8)	114(2)
C(14)–S(3)–C(15)	97(2)	S(7)–C(28)–C(27)	126(3)
C(14)–S(5)–C(20)	96(2)	S(8)–C(28)–C(27)	119(3)
C(21)–S(5)–C(27)	93(2)	S(7)–C(29)–C(34)	114(3)
C(26)–S(6)–C(27)	93(2)	S(8)–C(34)–C(29)	119(3)
C(28)–S(7)–C(29)	98(2)	S(9)–C(35)–C(36)	111(3)
C(28)–S(8)–C(34)	95(2)	S(10)–C(36)–C(35)	119(3)
C(35)–S(9)–C(41)	96(2)	S(9)–C(41)–S(10)	118(2)
C(36)–S(10)–C(41)	95(2)	S(9)–C(41)–C(42)	118(3)
C(42)–S(11)–C(48)	96(2)	S(10)–C(41)–C(42)	124(3)
C(42)–S(12)–C(43)	97(2)	S(11)–C(42)–S(12)	115(2)
S(1)–C(7)–C(12)	113(2)	S(11)–C(42)–C(41)	119(4)
S(2)–C(12)–C(8)	116(2)	S(12)–C(42)–C(41)	126(4)
S(1)–C(13)–S(2)	117(2)	S(12)–C(43)–C(48)	124(3)
S(1)–C(13)–C(14)	124(2)	S(11)–C(48)–C(43)	109(3)
S(2)–C(13)–C(14)	119(2)		

1.42(5) Å) and is close to that of neutral DBTTF (1.349(5) Å) [19]. These arrangements are consistent with the electronic reflectance spectra, which show two bands due to $DBTTF^{\ddagger}/DBTTF^{\ddagger}$ and $DBTTF^{\ddagger}/DBTTF^{0}$ charge transfer (c.t.) transitions, as described below.

The $[Sn_3Me_6Cl_8]^{2-}$ anion is constructed with the chloride-bridged trimerized dimethyltin(IV) skeletons (Fig. 3), which is a novel example for chlorodimethyltin(IV) anions. Sn(2) and Cl(3–6) are coplanar (±0.05 Å) with the averaged Sn(2)–Cl(3–6) distance of 2.66(3) Å and the C(3)–Sn(2)–C(4) linkage is almost linear (178(1)°). This geometry around the Sn(2) atom is very similar to those for the *trans*-$[SnMe_2Cl_4]^{2-}$ anion in $[pyridinium]_2[SnMe_2Cl_4]$ (Sn–C, 2.109(9); Sn–Cl, 2.603(2) and 2.625(2) Å) [20] and $[TTF]_3[SnMe_2Cl_4]$ (Sn–C, 2.098(18); Sn–Cl, 2.600(3) and 2.599(5) Å) [2]. In contrast to the linear C(3)–Sn(2)–C(4) linkage, C(1)–Sn(1)–C(2) and C(5)–Sn(3)–C(6) are appreciably bent (162(2) and 159(2)°, respectively). The averaged distances of Sn(1)–Cl(1, 2) and Sn(3)–Cl(7, 8) bonds are both 2.44(2) Å, while those of Sn(1)–Cl(3, 4) and Sn(3)–Cl(5, 6) bonds are 3.02(8) Å. Such a distorted octahedral configuration around the terminal tin atom corresponds to the neutral dimethyltin(IV) dichloride

coordinated by two chlorine atoms. The terminal Sn–Cl coordination bonds are considerably shorter than the intermolecular Sn---Cl contacts which were reported for [quinolinium] $[SnMe_2Cl_3]$ (3.486(7) Å) [22], [TTF] $[SnMe_2Cl_3]$ (3.367(6) Å) [2], and $SnMe_2Cl_2$ (3.54 Å) [23]. This is suggestive of a strong association of two $[SnMe_2Cl_4]^{2-}$ anions with a neutral $SnMe_2Cl_2$ molecule. The geometries around Sn(1) and Sn(3) are rather close to that of $SnMe_2Cl_2$·Ni(salen) (Sn–C, 2.12(1), 2.12(2); Sn–Cl, 2.443(4), 2.523(4) Å; C–Sn–C, 161.0(7)°) [21], where the tin atom is coordinated by two nitrogen atoms.

Dialkyltin(IV) chloride anions reported so far are $[SnR_2Cl_3]^-$ and $[SnR_2Cl_4]^{2-}$, which can be formed by the equilibrium reaction of SnR_2Cl_2 with the chloride ion in solution. It is noteworthy, however, that the present trimerized dimethyltin(IV) chloride anion can also be formed by the equilibrium reaction between $SnMe_2Cl_2$ and the chloride ion, and the formation of such a trimerized species may be suitable for the stabilization of the columnar packing of slender DBTTF molecules.

Donor molecules have an electrostatic interaction with the anion through sulfur and chlorine atoms; the closest contact between sulfur and chlorine atoms is 3.49(2) Å which is shorter than the sum (3.65 Å) [24] of van der Waals radii of both the atoms. This electrostatic interaction would lead to the charge transfer from the sulfur to the chlorine atom, which reflects on somewhat small binding energies of Sn 3d electrons as described below. Such electrostatic sulfur–chlorine interactions were observed also in $[TTF]_3[SnMe_2Cl_4]$ and [TTF] $[SnMe_2Cl_3]$ [2].

Electronic Properties of the Salts

The far–infrared spectrum of salt **2** has shown a weak band at 230 cm^{-1} and an intense broad band at 280 cm^{-1} both assignable to ν(Sn–Cl), which are characteristic of the trimerized $[Sn_3Me_6Cl_8]^{2-}$ anion. Similar spectra in appearance have been observed for salts **1**, **2**, **6**, and 7 (see Table IV). Salts **8**, **10**, and **11** have exhibited two strong ν(Sn–Cl) bands around 250 and 300 cm^{-1}, suggesting a pentacoordinate trigonal bipyramidal structure around the tin atom [2], as reported for $[NEt_4]$ $[SnMe_2Cl_3]$ (250 and 310 cm^{-1}) [25]. Salts **4** and **12**, however, have displayed one of the ν(Sn–Cl) bands at lower frequencies. This is suggestive of some lengthening of the Sn–Cl bonds owing to molecular interactions in the crystals.

Table V summarizes the binding energies of Sn $3d_{3/2}$ and $3d_{5/2}$ electrons determined from the X-ray photoelectron spectra (XPS) for the DBTTF, DBTSF, and TTT salts as well as some tin(IV) chloride compounds. Although the $[Sn_3Me_6Cl_8]^{2-}$ anion formally contains an $[SnMe_2Cl_4]^{2-}$ anion and two neutral $SnMe_2Cl_2$ molecules, only an XPS peak due to Sn 3d

TABLE IV. ν(Sn–Cl) Frequencies of DBTTF, DBTSF and TTT Salts

Salt	ν(Sn–Cl) (cm^{-1})		
1	219w	278s,br	
2	230w	280s,br	
4	217s,br	313s,br	
6	218w	282s,br	
7	220w	270s,br	
8	249s,br	288s	
10	258s,br	306s	
11	256s,br	296s,br	
12	208s,br	300s,br	307s

TABLE V. Binding Energies (eV) of the Sn Electrons in the Salts and Related Compounds, Determined from X-Ray Photoelectron Spectra

Compound	Sn $3d_{3/2}$	Sn $3d_{5/2}$
1	494.2	485.7
2	494.0	485.8
4	493.7	485.2
6	494.1	485.7
7	494.2	485.8
8	492.9	484.6
10	492.0	483.6
11	492.1	483.7
12	492.1	483.8
$SnMe_2Cl_2$	494.6	486.1
$SnEt_2Cl_2$	494.0	485.5
[TTF] $[SnMe_2Cl_3]$	493.9	485.3
[TTF] $[SnEt_2Cl_3]$	493.0	484.7

electrons has been observed, suggesting approximately averaged –2/3 charges on each tin atom. This is consistent with the observation that the binding energy of Sn 3d electrons in the $[Sn_3Me_6Cl_8]^{2-}$ anion is between those in $SnMe_2Cl_2$ (neutral) and [TTF] $[SnMe_2Cl_3]$ (the formal charge of the anion; –1) (see Table V). The binding energies in **2** and [TTF] $[SnMe_2Cl_3]$ are somewhat smaller than that of $[\overline{S(CH_2)_3SC}{=}NMe_2]$ $[SnMe_2Cl_3]$ (494.5 and 486.0 eV for Sn $3d_{3/2}$ and $3d_{5/2}$ electrons, respectively) [2]. This is due to a transfer of some negative charges from sulfur to chlorine atoms through the electrostatic interaction in the two former salts. The binding energies of Sn 3d electrons in the TTT salts with the $[SnMe_2Cl_3]^-$ anion are appreciably smaller than those in [TTF] $[SnMe_2Cl_3]$ as well as the [DBTTF]– and [DBTSF]– $[Sn_3Me_6Cl_8]^{2-}$ salts (Table V). Similarly, $[TTT]_{1.5}[SnEt_2Cl_3]$ exhibits the binding energies smaller than [DBTTF]– and [DBTSF]– $[SnEt_2Cl_3]^-$ salts (Table V). In view of these results, a sulfur–chlorine or sulfur–tin inter-

action may be more favorable in the TTT salts than in the corresponding DBTTF and DBTSF salts, presumably because of projecting sulfur atoms of the TTT molecule.

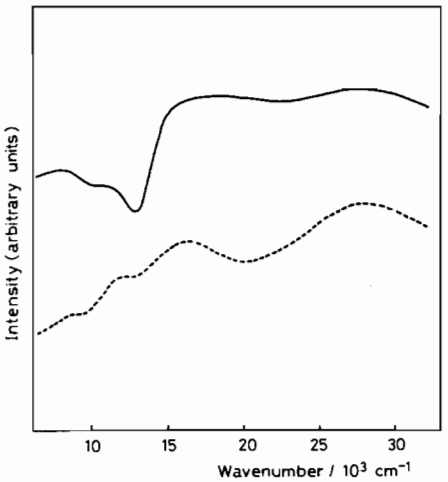

Fig. 4. Powder reflectance spectra of $[DBTTF]_{2.5}[Sn_3Me_6Cl_8]0.5MeCN$ (**4**) (———) and $[DBTSF]_{2.7}[SnCl_6]$ (**5**) (------).

Figure 4 shows the electronic reflectance spectra of **4** and **5**. The bands observed in the frequency region higher than 15000 cm^{-1} are attributed to local excitations of the $DBTTF^{\ddagger}$ or $DBTSF^{\ddagger}$ radical cation and the $DBTTF^0$ or $DBTSF^0$ molecule, as reported for the $DBTTF^{\ddagger}$ radical cation and the DBTTF molecule in solution [26]. The bands at 10800 and 8800 cm^{-1} of **4** are reasonably assigned to $DBTTF^{\ddagger}/DBTTF^{\ddagger}$ and $DBTTF^{\ddagger}/DBTTF^0$ c.t. transitions, respectively, by analogy with the electronic spectra of TTF and dimethyldibenzotetrathiafulvalene (DMDBTTF) salts, such as [TTF]Cl, $[TTF]Br_{0.79}$ [27], and $[DMDBTTF][BF_4]$ [28]. Although the remaining DBTTF salts have exhibited these two c.t. bands (Table VI), an unusual strong intensity of the $DBTTF^{\ddagger}/DBTTF^0$ c.t. band is characteristic of **4** which has an excellent electrical conductivity as described below.

Salt **5** also shows two bands due to the $DBTSF^{\ddagger}/DBTSF^{\ddagger}$ and $DBTSF^{\ddagger}/DBTSF^0$ c.t. transition in the region similar to that of the DBTTF salts. **6** and **7** exhibit spectra analogous to **5**, while **8** having no neutral DBTTF molecule displays only a band assigned to the $DBTSF^{\ddagger}/DBTSF^{\ddagger}$ c.t. transition. The c.t. band between the $DBTSF^{\ddagger}$ radical cations occurs at somewhat higher frequencies than that between the $DBTTF^{\ddagger}$ radical cations (see Table VI). This is consistent with the positively higher oxidation potentials of DBTSF ($DBTSF^{0/1+}$, +0.68; $DBTSF^{1+/2+}$, +1.11 V *vs.* s.c.e. in dichloromethane) than DBTTF ($DBTTF^{0/1+}$, +0.62; $DBTTF^{1+/2+}$, +1.02 V). The spectra of the TTT salts have shown the $TTT^{\ddagger}/TTT^{\ddagger}$ c.t. bands near 10000 cm^{-1}, while the $TTT^{\ddagger}/TTT^0$ c.t. band which probably occurs at lower frequencies than 8000 cm^{-1} [29] has not been measured. The spectral feature of the DBTTF, DBTSF, and TTT salts together with rather small resistivities of the salts except for **8** as described below suggests a columnar structure consisting of both $D^{\ddagger}/D^{\ddagger}$ and $D^{\ddagger}/D^0$ (D = donor molecule) interactions, as revealed from the crystal structure of **2**.

TABLE VI. Powder Reflectance Spectra of the DBTTF, DBTSF and TTT Salts

Salt	l.e. band of D[a] (10^3 cm^{-1})			c.t. band of D[a] (10^3 cm^{-1})	
				$D^{\ddagger}/D^{\ddagger}$ [a]	$D^{\ddagger}/D^0$ [a]
1	27.8	[b]	17.5	11.1	9.1
2	29.1	[b]	17.6	10.8	8.8
3	27.8	[b]	17.6	10.4	8.7
4	27.8	[b]	18.1	10.8	8.8
5	28.0	[b]	16.4	12.1	8.8
6	27.8	[b]	17.0	[b]	8.7
7	27.5	[b]	16.2	11.4	8.7
8	28.1	[b]	16.6	12.2	–
9	21.7	18.5	13.3	11.8	9.0
10	21.8	19.3	[b]	–	9.5
11	21.6	18.4	13.7	–	9.2
12	21.8	18.5	13.0	10.8	9.3

[a] D = DBTTF, DBTSF or TTT. [b] Obscured by the higher frequency bands.

Electrical Resistivity

Figure 5 illustrates the temperature dependence of electrical resistivities of the salts. The resistivities at 25 °C and the activation energies for electrical conduction are summarized in Table VII. All the

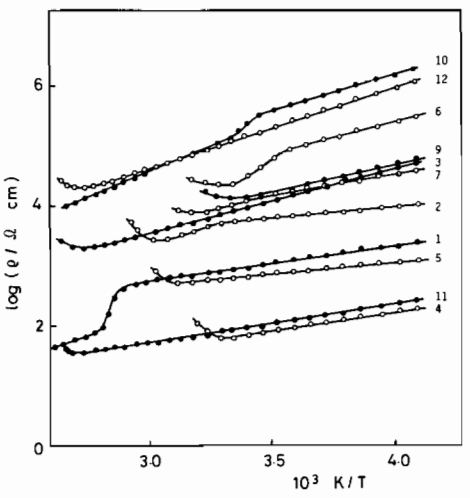

Fig. 5. Temperature dependence of electrical resistivities of the salts.

TABLE VII. Electrical Resistivities (ρ) and Activation Energies (E_a) of the DBTTF, DBTSF and TTT Salts

Salt	ρ_{25} °C (Ω cm)	E_a (eV)
1	8.3×10^2	0.13
2	5.6×10^3	0.057
3	1.2×10^4	0.17
4	6.1×10^1	0.13
5	6.1×10^2	0.082
6	4.0×10^4	0.24
7	1.0×10^4	0.16
8	$>10^8$	
9	7.7×10^3	0.23
10	1.5×10^5	0.32
11	8.3×10^1	0.14
12	1.3×10^5	0.26

salts except for **8** behave as typical semi-conductors in the temperature range −30 to +40 °C. Although **8** contains the $DBTSF^{\ddagger}$ radical cation but no neutral DBTSF, the other salts prepared in this study involve both the donor radical cation and the neutral molecule, exhibiting rather small resistivities because of the presence of an effective electrical conduction column; in particular, the resistivities of **4** and **11** are extremely small. Previously, $[DBTTF]_8[SnCl_6]_3$ was reported to exhibit a metallic conductivity [4]. The DBTSF analog **5**, however, behaves as a semiconductor with somewhat large resistivity, although the activation energy is small.

Salt **1** exhibits an irreversible change of resistivity upon heating around 40 °C. This may be due to a thermal redox reaction, since more of the neutral DBTTF molecule has been detected in the salt after thermal reaction.

Supplementary Material

Atomic thermal parameters and observed and calculated structure factors have been deposited with the Editor-in-Chief.

Acknowledgements

We wish to express hearty thanks to Professor Kazumi Nakatsu of Kwansei Gakuin University, Nishinomiya, Hyogo, for the use of the X-ray diffractometer and the programs for the structure solution and refinement. This work was partially supported by the Kurata Research Grant, for which we thank the Kurata Foundation.

References

1 K. Kondo, G. Matsubayashi, T. Tanaka, H. Yoshioka and K. Nakatsu, *J. Chem. Soc., Dalton Trans.*, 379 (1984).
2 G. Matsubayashi, K. Ueyama and T. Tanaka, *J. Chem. Soc., Dalton Trans.*, 465 (1985).
3 K. Ueyama, G. Matsubayashi, R. Shimizu and T. Tanaka, *Polyhedron, 4*, 1783 (1985).
4 (a) L. S. Veretennikva, R. N. Lyubovskaya, R. B. Lyubovskii, L. P. Rozenberg, M. A. Simonov, R. P. Shibaeva and M. L. Khidekel, *Dokl. Akad. Nauk SSSR, 241*, 862 (1978); (b) R. N Lyubovskaya, R. B. Lyubovskii, U. A. Merzhanov and M. L. Khidekel, *Sov. Phys. JETP, 49*, 720 (1979).
5 G. Matsubayashi, R. Shimizu and T. Tanaka, *Chem. Lett.*, 973 (1985).
6 J. Nakayama, *Synthesis, 38*, 168 (1975).
7 I. Johannsen, K. Bechgaar, K. Mortensen and C. Jacobsen, *J. Chem. Soc., Chem. Commun.*, 295 (1983).
8 I. V. Krivoshei, V. P. Babiyczuk, I. M. Guella, I. F. Golovkina, N. V. Mansia, V. A. Starodub and S. A. Chueva, *Phys. Status Solidi A, 50*, K197 (1978).
9 Z. S. Ariyan and L. A. Wiles, *J. Chem. Soc.*, 1725 (1962).
10 I. Wharf and D. F. Shriver, *Inorg. Chem., 8*, 914 (1969).
11 S. Araki, H. Ishida and T. Tanaka, *Bull. Chem. Soc. Jpn., 51*, 407 (1978).
12 K. Ueyama, G. Matsubayashi and T. Tanaka, *Inorg. Chim. Acta, 87*, 143 (1984).
13 G. Matsubayashi, K. Kondo and T. Tanaka, *Inorg. Chim. Acta, 69*, 167 (1983).
14 'International Tables for X-Ray Crystallography', Vol. 4, Kynoch Press, Birmingham, 1974.
15 C. K. Johnson, 'ORTEP-II', a FORTRAN thermal-ellipsoids program for crystal structure illustrations, ORNL. 5183, Oak Ridge, 1976.
16 R. P. Shibaeva, L. C. Rozenberg and P. M. Lobkobska, *Kristallografiya, 25*, 507 (1980).
17 T. J. Emge, F. M. Wiygul, J. S. Chappell, A. N. Bloch, J. P. Ferraris, D. O. Cowan and T. J. Kistenmacher, *Mol. Cryst. Liq. Cryst., 87*, 137 (1982).
18 M. Tanaka, M. Honda, C. Katayama, H. Fujimoto and J. Tanaka, *Chem. Lett.*, 219 (1985).
19 R. P. Shibaeva, R. N. Lobkovskaya and V. N. Klyuev, *Cryst. Struct. Commun., 11*, 835 (1982).
20 L. E. Smart and M. Webster, *J. Chem. Soc., Dalton Trans.*, 1924 (1976).
21 M. Calligaris, L. Randaccio, R. Barbieri and L. Pellerito, *J. Organomet. Chem., 76*, C56 (1974).
22 A. J. Buttenshaw, M. Duchene and M. Webster, *J. Chem. Soc., Dalton Trans.*, 2230 (1975).
23 A. G. Darris, H. J. Milledge, D. C. Puxley and P. J. Smith, *J. Chem. Soc. A*, 2862 (1970).
24 L. Pauling, 'The Nature of the Chemical Bond', 3rd edn., Cornell University Press, Ithaca, New York, 1960, p. 249.
25 I. R. Beattie, F. C. Stokes and L. E. Alexander, *J. Chem. Soc., Dalton Trans.*, 465 (1973).
26 S. Hünig, G. Kiesslich, H. Quast and D. Scheutzow, *Liebigs Ann. Chem.*, 310 (1973).
27 J. B. Torrance, B. A. Scott, B. Webster, F. B. Kaufman and P. E. Seiden, *Phys. Rev., B, 19* 730 (1979).
28 C. Tanaka, J. Tanaka, K. Dietz, C. Katayama and M. Tanaka, *Bull. Chem. Soc. Jpn., 56*, 405 (1983).
29 T. Inabe and Y. Matsunaga, *Bull. Chem. Soc. Jpn., 51*, 2813 (1978).